Lawrence Berkeley National Laboratory
LBL Publications

Title
Extracting Natural Biosurfactants from Humus Deposits for Subsurface Engineering Applications

Permalink
https://escholarship.org/uc/item/3z79x6xg

Journal
Energy & Fuels, 31(11)

ISSN
0887-0624

Authors
Wan, Jiamin
Tokunaga, Tetsu K
Dong, Wenming
et al.

Publication Date
2017-11-16

DOI
10.1021/acs.energyfuels.7b02203

Peer reviewed

eScholarship.org Powered by the California Digital Library
University of California

Extracting Natural Biosurfactants from Humus Deposits for Subsurface Engineering Applications

Jiamin Wan*, Wenming Dong, Yongman Kim, and Tetsu K. Tokunaga

Energy Geosciences Division, Earth and Environment Sciences Area, Lawrence Berkeley National Laboratory, 1 Cyclotron Road, Berkeley, California 94720

Corresponding author: Jiamin Wan, 510-486-6004, jwan@lbl.gov

Keywords: natural biosurfactants, foams, viscosity, EOR, non-water fracturing

TOC Art:

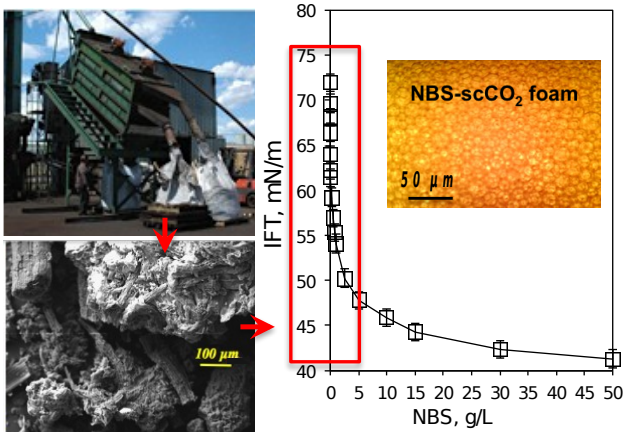

Supporting Information: video on $scCO_2$-foam flow

Abstract

More environmentally benign, economical, and effective surfactants and additives are increasingly needed in engineering subsurface energy recovery processes. Biosurfactants have some advantageous over chemically synthesized surfactants, however the high costs of microbial-biosynthesis prohibits their applications in subsurface engineering. Here we propose to use already naturally formed biosurfactants contained within Earth's abundant humus deposits for subsurface engineering applications. Humus is plentiful, inexpensive, and readily available. We collected humus samples of different types from four different geographic regions, and developed a simple method for extracting natural biosurfactant (NBS) used only four common chemicals. The average NBS extraction yields are 17±6 % of the raw humus tested. No significant differences in elemental composition and functional group chemistry were found among the NBS extracted from humus of different origins, suggesting that mostly any humus deposits can be used as the raw material for NBS. Measurements of interfacial tensions between air-water and supercritical (sc) CO_2-water interfaces indicate that the NBS is a highly effective surfactant. NBS has good foaming ability. In our preliminary tests with only 0.5 mass % NBS in the aqueous phase (no other additives), the NBS generated scCO_2-in-waster foams reached 90% foam quality with the foam apparent viscosities up to 30 cP. These results suggest that NBS merits further research and development as a potential new technology for industrial scale subsurface energy production.

INTRODUCTION

Using alternative fluids (e. g., CO_2, N_2, and natural gas) to replace water in hydraulic fracturing has become an attractive next step to

resolve the issues resulted from using water-based fracturing fluids, including wastewater generation and treatment, and water formation damage from water blocking of shale pores[1]. The primary barrier of using these alternative fluids is their very low viscosity, much lower than that of water. Yet CO_2 has the advantage of miscibility with oil under elevated pressure, and this has been driving the technology of CO_2 enhanced oil recovery (EOR). However the low viscosity of CO_2 causes the injected CO_2 bypass the remaining oil[2]. The thickeners for directly thickening CO_2 have been developed and tested in laboratories, yet the associated issues of high costs and toxicity prevent their field application[2-3]. The use of surfactant-stabilized CO_2 foams/emulsions is more promising for CO_2 mobility control in EOR[4]. Droplets of $scCO_2$ separated by surfactant-stabilized lamella exhibit significantly increased effective viscosity. Advancements on improved foam quality and viscosity have been made in the recent years with newly designed surfactants and some with nanoparticles as stabilizers[5]. In hydraulic fracturing, although liquid (L) CO_2, LN_2, and liquid hydrocarbons have been tested and applied in the field as fracturing fluids, the results suggested that higher viscosity is needed for a fracturing fluid to initiate and propagate high quality fracture networks, and to transport and place proppants into the fractures[1]. Some oil-in-water emulsions and gas-in-water foams have been developed to obtain desired viscosities, but their efficiency, costs, and environmental concerns associated with surfactants for generating optimal properties remain key challenges.

Biosurfactants have been synthesized for applications in such as cosmetic and pharmaceutical industries[6]. The high costs associated with biosynthesizing and downstream purification prohibits their use in large-scale subsurface engineering applications. Organic-rich soils and sediments are common, and some of these deposits (e.g., peat, leonardite) are sufficiently concentrated that they are mined and

marketed as soil amendments (http://minerals.usgs.gov/minerals). Importantly, many components in natural organic materials common in soils and organic-rich sediments possess both hydrophilic and hydrophobic moieties[7], hence can readily accumulate at interfaces. Humus is regarded as a refractory fraction of soil organic matter, a mixture of highly heterogeneous and complex polymers, created by microorganisms through degradation of plants, microbes and animal remains. Humus plays essential roles in benefiting soil fertility and structure, and has been studied extensively due to its importance in agriculture, soil chemistry, microbial ecology, and environmental sciences[7]. Methods for fractionating humic substances are well developed, although rather generic because of the highly complex structure and aggregation into supramolecular associations[8,9]. A large fraction of humic acid is lipid-like, including characteristics of fats, waxes, sterols, glycerides, and phospholipids. The micelle-like behavior of humic acids in solutions reflects their amphiphilic/surfactant properties[10]. This paper reports on our exploration of humic substances as a source for natural biosurfactants (NBS) useful for stabilizing emulsions and foams for potential subsurface engineering applications. Extraction and characterization of NBS will be described, followed by results of interfacial tension (IFT) measurements on NBS solution-air and NBS solution-scCO_2 interfaces, and initial measurements of effective viscosities of NBS-stabilized scCO_2 foams.

EXPERIMENTAL

Raw materials for NBS extraction. The raw materials from which NBS was extracted included natural humus, peat and Leonardite from four different sources (Figure 1): North Dakota Leonardite (Leonardite Products, LLC, Williston, ND), Florida Peat (Organic Products Co. Orlando, FL), Aldrich Leonardite (Cat. # H16752, http://www.sigmaaldrich.com, from a deposit in Germany), and humic

material extracted from peat (International Humic Substances Society, Pahokee Peat from Florida, Cat. # 2BS103P, http://humic-substances.org). The samples were used as received (< 2.0 mm). Four chemicals were used in NBS extraction: sodium hydroxide, hydrochloric acid, benzene, and methanol. These chemicals were all Reagent grade, but Technical/Industrial grade chemicals are expected to be suitable.

NBS extraction. The humus samples (< 2 mm, as received) were oven-dried at 75 ˚C for 24 hours. A Soxhlet extraction was applied to the samples because it efficiently recycles small amounts of solvent to dissolve a larger amounts of substrate[11]. We used a simple three step method (modified from Chilom et al.[9b]) that involved: pretreatment, solvent-extraction, and alkaline-cleaning. In Step 1, we compared alkaline- and acid- pretreatments against no pretreatment. In alkaline-pretreatment 0.3 M NaOH solution was added to the substrate at a liquid to solid ratio of 10 mL/g in a bottle, and mixed overnight on an orbital shaker. The undissolved fraction was discarded; the supernatant solution pH was adjusted to within 1 to 2 with 6 N HCl, and equilibrated overnight. After the precipitate was washed using water, dried at 75 ˚C, and weighted, it was ready to be used for Step 2. As an alternative pretreatment method, acid was used to remove mineral solids. 1.0 N HCl solution was added at a liquid to solid ratio of 10 mL/g, mixed in a bottle on an orbital shaker overnight, decanted, rinsed with deionized water, and oven-dried for the next step. For the non-pretreatment approach, dry raw materials were directly used. In Step 2, the treated or non-treated material was subjected to Soxlet extraction with a solvent:solid ratio of 15:1 mL/g. The solvent used was a mixture of benzene and methanol (3:1 volumetric ratio), at 60 ˚C for ~72 hrs. The remaining solid phase was discarded; the solvent was evaporated away and condensed for later reuse; and the extracts were harvested for Step 3. The solvent-extracted fraction was lastly

subjected to alkaline cleaning. This final step served to remove the highly hydrophobic fraction that is insoluble in alkaline (0.1 M NaOH) solution. The solution to solid ratio of 30 mL/g was mixed in a bottle and shaken overnight, then centrifuged to remove the residual solids. The remaining supernatant containing NBS was ready for used as the stock solution after determine its NBS concentration. Dry NBS can be obtained by adjusting the solution pH to 1-2 with 6 N HCl, equilibrating overnight, centrifuge to remove the supernatant, and oven drying to recover the precipitate.

NBS chemical composition and function group analyses. The solid NBS and intermediate products in the extraction process were analyzed for their chemical composition (C, H, N, O, S%) and function groups. The CHNOS analyses were performed by ALS Environmental Micro-elemental Laboratory (Tucson, Arizona. http://www.caslab.com/Tucson-Laboratory/) using PerkinElmer 2400 CHNS/O Series II combustion analyzer. To determine ash content, thermo gravimetric analyses (TGA) was used (TA Instruments SDT-Q600). To determine molecular functional groups, FTIR spectra were obtained with a Thermo Nicolet iS50 spectrometer. ATR spectra were collected with a MCTA detector; resolution of 2 cm^{-1}, 64 scans per sample, over the range of 400 - 4000 cm^{-1}.

Air-water and $scCO_2$-water interfacial tension measurements. The interfacial tensions (IFT) at air-NBS solution interfaces were measured using the Du Nouy ring method (K11, Kruss.com) under ambient conditions (23 ˚C, atmospheric pressure). For measuring $scCO_2$-NBS solution IFT, the pendant drop method was performed at 12 MPa and 45˚C. A high-pressure chamber with two transparent windows allows illumination and imaging of a fluid droplet formed and equilibrated within $scCO_2$[12]. The chamber was instrumented with a

pressure transducer, a thermocouple, and a movable needle used to inject the liquid droplet. Two high-pressure syringe pumps (Teledyne ISCO, 500D/65D) were used to control pressure and deliver $scCO_2$ and aqueous solution. Both $scCO_2$ and water are contained in the chamber to maintain mutual solubility equilibrium, after which a NBS solution droplet was introduced into the $scCO_2$ phase. Evolution of the shape of the droplet was monitored using high-resolution time-lapse photography. Because the shape of a droplet changes with time, only equilibrium images of droplets (5 minutes to 2 hours) were used for generating the IFT data. For each reported IFT value, at least 3 droplets were measured, with at least 5 images analyzed per droplet.

NBS stabilized foam generation. We first used a simple method to generate air-in-water foam for evaluating the foam generation capabilities of all the NBS samples, and to identify optimal conditions (NBS concentrations, pH and ionic strength) for generating $scCO_2$-in-water foams (Figure 2). In generating air-in-water foams, 2 mL of NBS solution was put in a small glass vial, sealed with a lid, and vigorously shaken for 1 minute. The height of the foam in the jar was recorded over time. We then selected the most promising set of parameters from the air-foam testing to generate $scCO_2$-foams using our laboratory-built foam generator and rheometer (Figure 2).

The foam generator consists of a stainless steel column (1.0 cm ID and 30 cm long) packed with sand (Unimin sand, 106 to 212 μm, permeability = 4.4×10^{-12} m^2, porosity ~0.38, pore volume 1.45 mL). Two high-pressure pumps (Teledyne, ISCO D-Series syringe pumps) were separately filled with one of the two fluids, NBS aqueous solution and $scCO_2$. With the two syringe pumps operated in parallel, the two fluids were co-injected into the sand column under selected volumetric flow ratios of 1:4 to 1:9, and combined flow rates ranging from 6 to 36 mL per minute, while the downstream backpressure (varied between

~8.5 and ~11 MPa) was controlled with a third ISCO pump. The rheometer (viscometer) was a capillary tube (stainless steel, 760 μm ID, 3.3 m long, coiled into a helix with a 0.17 m diameter), located immediately downstream of the sand column. Two pressure transducers at the ends of the coil allowed measurements of pressure drops and effective viscosities during flow. Prior to the foam tests, the rheometer was calibrated by pumping water at steady flow rates and correlating the measured pressure differential acting across the coiled capillary with the known viscosity water for the given temperature and average total pressure. These calibration measurements were found to be in good agreement with predictions for viscous flow in coiled tubes[13]. The pressure drops across the capillary tube measured during foam flow were then used to calculate apparent viscosities. The main components for the experimental system were kept within an insulated enclosure with temperature controlled at 45 ± 1°C. The morphology of foams was visually monitored through the viewing window of a horizontally oriented Jerguson high pressure gage (Series 40, rated to 134 MPa at 38 ˚C), located downstream of the rheometer. Microscope images of finer scale foam morphology were obtained by diverting effluents into a glass micromodel (Micronit Microfluidics) [21], mounted on an inverted microscope (Zeiss, Observer Z1.m, with AxioCam MRc5 CCD camera). Pressures ranging from 8.5 to 11 MPa were used for the foam tests, with the majority conducted in the 8.5 to 9.0 MPa range in order to remain within the 10.0 MPa pressure limit of the micromodel.

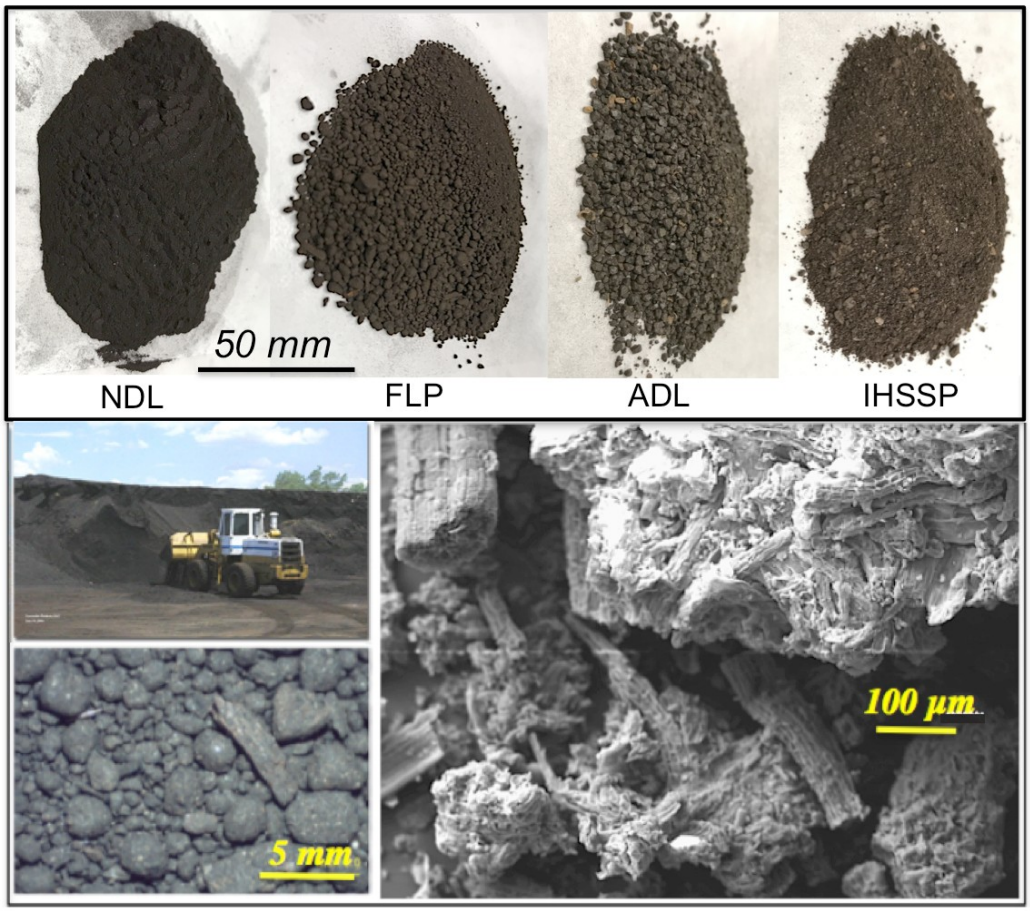

Figure 1. Photographs of raw materials (humus) tested for NBS extraction. The upper panel photographs show samples as received from different sources. The magnified images (lower panels) show morphology of remnant biological structure (sample FLP). The photograph with a loader and stockpile provides a snapshot of the field recovery of the raw material (photo with permission from Leonardite Products, LLC, Williston, ND).

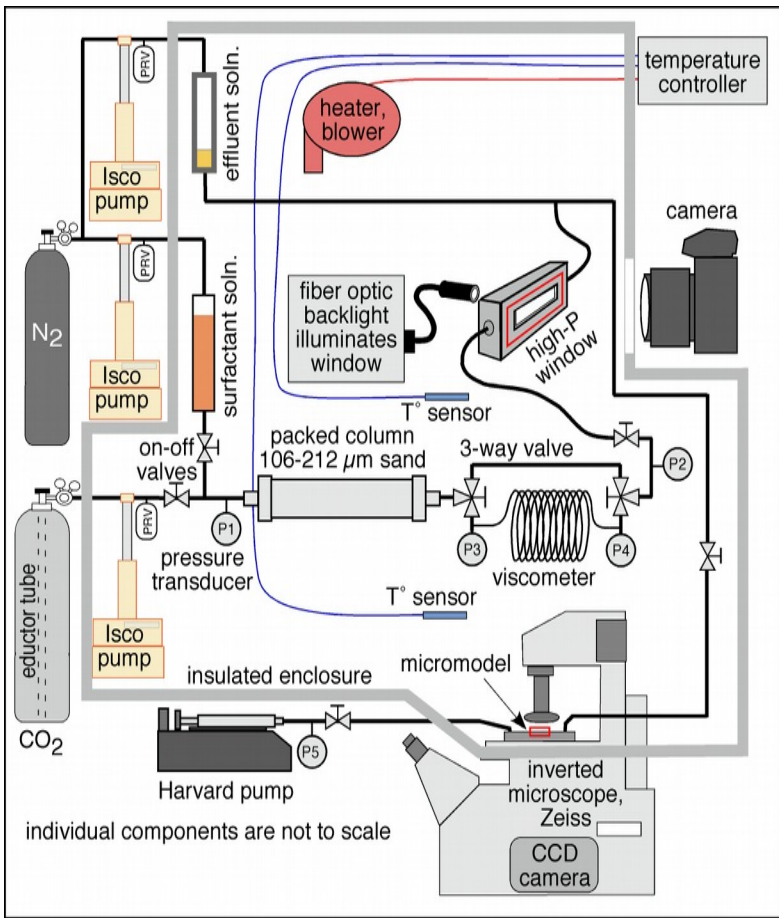

Figure 2. Schematic diagram of foam generator and rheometer for supercritical fluid foams. The foam can be studied visually through the window of the high-pressure viewing chamber and microscope at the downstream of the viscometer.

RESULTS AND DISCUSSIONS

NBS extraction and yields. Photographs of four humus samples used in this study are shown in Figure 1 with the magnified images (bottom panel) showing remnants of degraded organic matter. The NBS extraction yields from these humus samples are summarized in Table 1, based on dry weights of raw humus. The product of alkaline-pretreatment is called humic acid (HA). Because HA is a commonly recognized organic matter fraction of soils, we also reported the

extraction yields of HA, and NBS yields relative to HA. The yielded HA vary substantially, 58±9%. The solvent-extracted fraction accounts for 35.8 ±1.7 % of HA, and the NBS yields accounts 30.0 ±2.8% of the HA, and 17.3 ±2.6% of the raw humus. These are average values obtained from the four raw humus samples tested shown in Table 1. The most important information here is that a large percentage (~17%) of the natural humus is extractable surfactant. It is also important to know that the NBS yields accounts for 30.0 ±2.8% of HA, consistently from samples of different origins. The cost of NBS will largely associate with the extraction process instead of raw material, therefore high HA content should be considered as a criterion in selecting humus as the starting material. The final alkaline-cleaning step removed a small highly hydrophobic fraction (~6% of HA) that does not dissolve in alkaline solution. The pretreatment of acid-wash resulted no significant but slightly (up to 2%) higher yields. Because the acid-pretreatment (omitting first obtaining HA) leaves a larger unwanted fraction to Step 2, we decided not continue the acid-pretreatment approach. We also tested direct solvent-extraction without pretreatment. The results showed substantial reduced yields and increased extraction time, with one example presented at the last row of Table 1. Further studies on NBS extraction are necessary to optimize yields and quality. Many factors affect production yields and functions of the NBS, including extraction procedures and solvent selection. Today advanced separation technologies are widely used in industries [14], and a wealth of literature exists on methods development for shortening extraction time, reducing solvent usage, and simplifying procedures, including extraction under elevated pressure and temperature[15], microwave-assisted, ultrasound-assisted, and supercritical CO_2 extractions[16].

It should be noted that no further filtration or refinement of the NBS was performed for removal of colloids and nanoparticles likely present in the final extracts. Such separation would add to the cost of

285NBS extraction. Moreover, the presence of nanoparticles in the NBS
286may enhance the stability of CO_2-water interfaces, as demonstrated in
287other recent studies.
288

Table 1. NBS extraction yields (relative to dry raw humus and HA).

Sample ID	Sample Origin	[1]HA% from humus	[2]Solvent ext.% from HA	NBS% from HA	NBS% from humus
NDL	North Dakota (Leonardite Products, LLC, Williston, ND)	62.8	36.8	32.6	20.5
FLP	Florida (Organic Products Co. Orlando, FL)	43.3	37.4	30.7	13.3
ADL	Aldrich (Cat. # H16752)	68	33	25.2	17.1
IHSSP	IHSS (Cat. # 2BS103P)	57.6	36.1	31.4	18.1
IHSSP	IHSS (Cat. # 2BS103P)	no-pretreatment	NA	NA	11.6

[1]*Alkaline-pretreatment resulted humic acid (HA).*

[2]*Solvent extracts from HA.*

Chemical composition and functional group characteristics. The C, H, N, O, S% composition data are normalized by assuming that the sum of C, H, N, S, O, moisture, and ash = 100%; and that O% = 100% - sum of [CHNS, moisture, ash] (**Table 2)**. The data include examples from two complete sets of intermediate and final products including HA from alkaline-pretreatment, the discarded solvent-extraction fraction, the retained solvent-extraction fraction, alkaline-cleaning discarded fraction, and NBS. In addition, the compositions of another two NBS fractions and ash contents from TGA are presented for comparison (lower section of Table 2). Although there is considerable variability, the discarded solvent-extraction fraction had more hydrophilic components that contain more N and O groups from HA. The alkaline-cleaning discarded hydrophobic non-polar aliphatic groups containing higher C-H. The final NBS contain 53.1 ±6.5% C, 4.4 ±0.7 H%, 30.8 ±1.4% O (in COOH and OH), and high C and H in phenolic rings.

The FTIR spectra from all extraction steps for NDL as an example

are shown in Figure 3a. The spectra of NBS extracted from all four humus samples are presented in Figure 3b. The broad band in the vicinity of 3300 cm^{-1} is attributed to O-H and N-H stretching. The peaks at 2920 and 2850 cm^{-1}, and 1450 cm^{-1} represent C-H stretch of aliphatic groups. The clear peaks 1720 and 1610 cm^{-1} are mostly contributed by aromatic C, carbonyl groups in ketones, aldehydes, carboxylic acids, and their functional derivatives. The peak near 1225 cm^{-1} may be the contributions of C–O and OH of COOH, C–O of aryl ethers and phenols[17]. In Figure 3a, the solvent-extraction discarded fraction (green spectrum) contains more hydrophilic (3300 cm^{-1}) groups, and the solvent-kept fraction (purple spectrum) contains relatively more amphiphilic C. The alkaline-cleaning step resulted in removal of a significant fraction of insoluble aliphatic C-H, as shown in blue spectrum with strong aliphatic bands at 2920 and 2850 cm^{-1}, as well as a distinct peak at 1450 cm^{-1}. These spectral trends are consistent with the chemical composition data in Table 2; showing that the solvent-extraction removed fractions higher in N and O, and that the alkaline-cleaning removed more C and H, and less O and N relative to the NBS fraction. It is important to note that different source material types (peat or leonardite) and geographic locations of the source humus do not result in significant differences in the overall chemical compositions and function group chemistry of their extracted NBS (Table 2 and Figure 3b), although variation in some detailed features is evident.

Table 2. Chemical compositions of NBS and their intermediate products*

Sample	C%	H%	N%	O%	S%	H2O%	Ash%	C:N	C:H	C:O
NDL-pret-HA	51.5	4.7	2.9	31.9	0.3	5.5	3.5	17.7	10.9	1.6
NDL-solv-disc	57.0	5.2	2.8	28.5	0.3	4.7	1.8	20.1	11.0	2.0
NDL-solv-kept	53.6	5.1	2.7	26.9	0.3	6.2	5.5	19.9	10.4	2.0
NDL-clean-disc	66.4	8.2	1.2	16.6	0.1	2.5	5.1	54.8	8.1	4.0
NDL-NBS	58.0	5.3	2.4	29.6	0.3	4.7	0.1	24.1	11.0	2.0
FLP-pret-HA	55.4	4.2	1.6	31.7	0.2	3.6	3.5	35.8	13.1	1.8
FLP-solv-disc	55.2	3.9	1.6	32.6	0.2	3.7	3.1	34.1	14.3	1.7
FLP-solv-kept	57.6	5.1	1.1	29.3	0.2	4.2	2.8	52.4	11.4	2.0
FLP-clean-disc	70.1	8.2	0.7	17.7	0.1	3.3	0.0	97.4	8.5	4.0
FLP-NBS	57.0	4.9	1.1	29.7	0.2	5.4	1.9	51.3	11.6	1.9
IHSSP-NBS	55.7	4.1	1.3	33.0	0.6	5.9	0.0	42.9	13.6	1.7
ADL-NBS	41.9	3.4	0.9	30.7	0.5	5.5	17.6	48.7	12.2	1.4
FLP-NBS	57.0	4.9	1.1	29.7	0.2	5.4	1.9	51.3	11.6	1.9
NDL-NBS	58.0	5.3	2.4	29.6	0.3	4.7	0.1	24.1	11.0	2.0

**Assuming the sum of C, H, N, S, O, moisture, and ash = 100%; and O % = 100% - sum of CHNS-moisture-ash. HA= humic acid; solv-disc = discarded fraction from solvent extraction; solv-kept = solvent extracted fraction; clean-disc = discarded fraction, non-dissolvable in alkaline solution; NBS = solvent extracted and alkaline solution dissolvable fraction.*

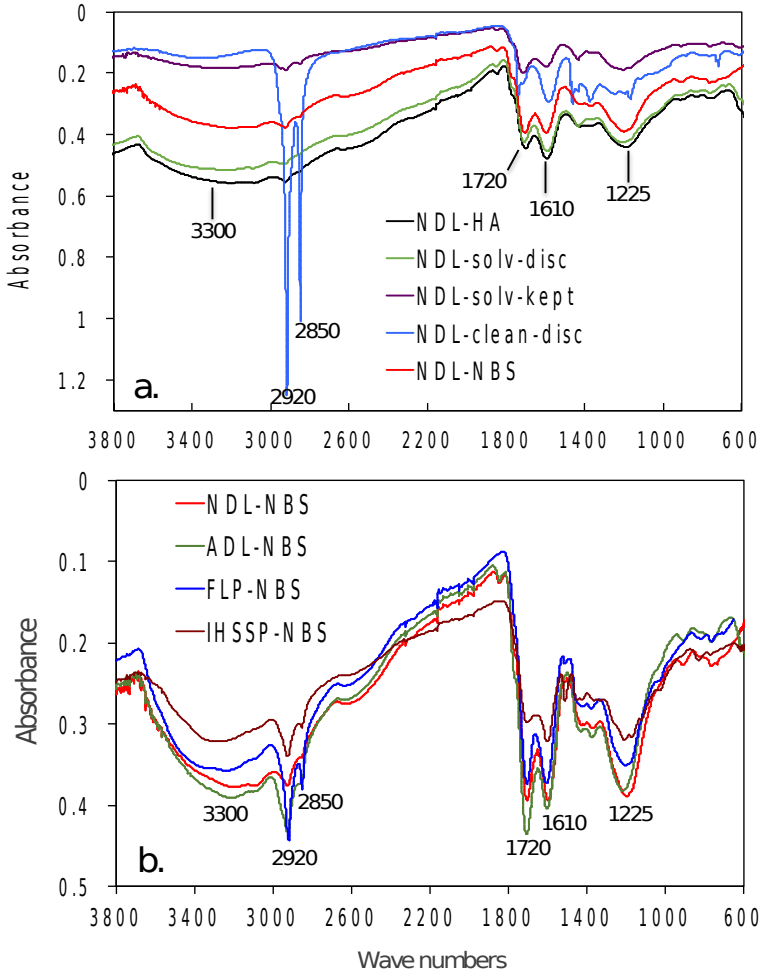

347

348**Figure 3.** FTIR spectra of intermediate and final extraction products.
349**(a)** A complete set of spectra of intermediate and final products from
350NDL raw humus, including HA, solvent-extraction discarded, solvent-
351extraction kept, alkaline-cleaning discarded and the NBS. **(b)** Spectra
352of NBS extracted from four humus samples of different origins.

353

NBS effects on air-water and $scCO_2$-water interfacial tensions. The measured interfacial tension (IFT) values of air-NBS solutions under varying NBS concentrations are presented in Figure 4. The measurements for the four NBS samples of different origins show that IFT values rapidly decrease as NBS concentration increases within the lower concentration range, NBS < ~0.2 mass %, and that IFT still continues to decreases with concentration afterwards. Different from synthetic surfactants, there is no clear critical micelle concentration (CMC) found for the various NBS samples. The extent of decreased IFT values is similar to those achieved with synthetic surfactants. For example, at 25˚C, Enordet AOS 1416 reaches an IFT about 32 mN/m, and Chaser SD1000 reaches an IFT of 47-40 mN/m at their micelle concentrations[18]. Although there are clear differences among the four NBS samples, in-depth studies of these samples are beyond the scope of this paper. It is worth noting that the greatest reduction in IFT occurs under alkaline conditions (pH ≥ 9.0) The surface activity of NBS has a relatively high tolerance to salinity, decreasing as salinity increases to ≥ 1.0 M (NaCl).

Before measuring IFT between $scCO_2$ and NBS solutions, the integrity of the high-pressure IFT measurement apparatus and procedure were first tested through measuring the IFT between air and pure water. Our measured air-pure water IFT at 22.5˚C was 72.3 mN/m, in good agreement with the value of 72.4 mN/m obtained with a regression relation from a standard reference[19]. Another test was done on the $scCO_2$-pure water IFT, where our measurement at 12.0 MPa and 45 ˚C yielded 24.2 mN/m, compared with 22 mN/m interpolated from measurements at slightly different P-T conditions[20]. Figure 5a shows an example image obtained during the IFT measurements: a NBS-solution droplet suspended within $scCO_2$ in the high-pressure chamber. The IFT value was calculated based on the curvature of the droplet at the equilibrium state. For each data point triplicate measurements (3

droplets) were conducted. NBS reduced IFT of $scCO_2$-NBS solutions down to 11.2 and 8.7 mN/m for the FLP-NBS at the NBS concentrations 0.5% and 1.5%, respectively, respectively (Figure 5a). The data of NDL-1 and NDL-2 are from the alkaline- and acid-pretreated procedures, respectively. The different origins of the raw humus from which the NBS was extracted had relatively small influence on the extent of the IFT reduction (Figure 5b).

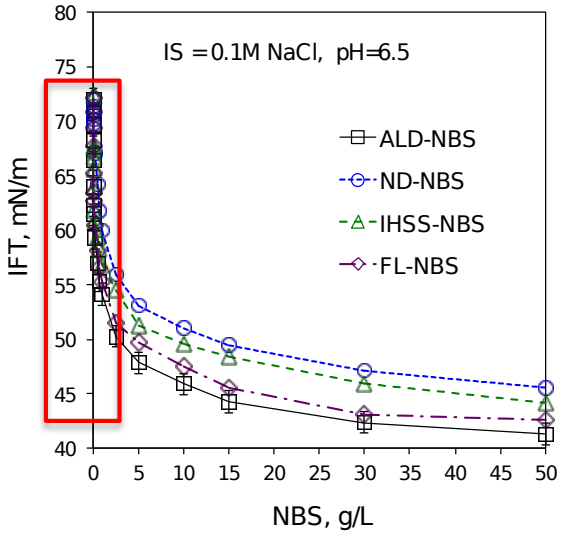

Figure 4. Measured air-NBS solution interfacial tension (IFT). All solutions contained 0.1 M NaCl and pH 6.5. The measurements were conducted at 22.5 ± 0.5 ˚C.

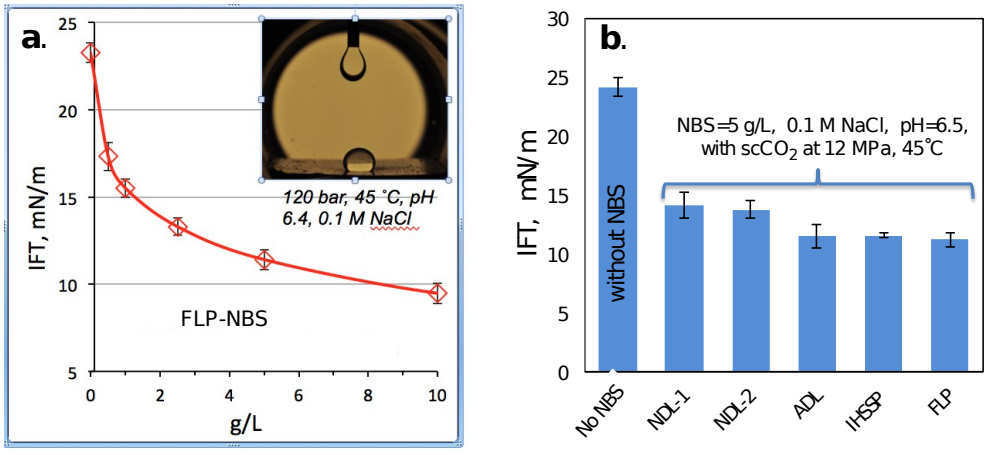

Figure 5. Measuring interfacial tensions between $scCO_2$ and NBS solutions. (**a**) Example image of NBS solution droplet suspended within $scCO_2$ at 12.0 MPa and 45˚C. Each IFT value was calculated from an image at the equilibrium state. (b) IFT values at NBS = 0.5g/L, pH 6.5, and 0.1 M NaCl for NBS samples of different origins. The NDL-1 and NDL-2 samples are from the alkaline- and acid-pretreated procedures, respectively.

Generating NBS foams. A simple air-in-water foam method was first used for screening of NBS foaming ability and identifying foaming conditions for the $scCO_2$-foam experiment. Aqueous solutions were prepared with NBS of different origins, concentrations, pH and ionic strength. The photographs in Figure 6 show examples of NBS stabilized air-in-water foams generated by vigorously shaking sealed vials containing small amounts of NBS solution for 1 minute under ambient conditions. The NBS extracted from different original source materials all showed efficient foaming ability (Figure 6a), with no significant/systematic differences observed for foam height and duration. Note that the sample “Minnesota” (Peat Inc., Elk River, MN) in the photograph was not discussed in other sections because data are incomplete for this sample. Using this method, we determined that ~ 0.5% is the optimal NBS concentration (being both low and efficient). Increased NBS concentrations yielded longer lasting foams, but did not significantly increase the foam height. Decreased NBS concentration (down to 0.1%) resulted in significantly reduced foam height and duration. For the ionic strength effect, no significant differences were observed between 0.1 and 0.5 M, but NaCl concentrations higher than 1.0 M reduced foam height and stability. We observed reasonable foaming ability over a wide range of pH from 3 to 9. While these tests provide information for screening stability ranges, more quantitative studies of the aforementioned parameters will be needed for developing applications suitable for specific environmental conditions.

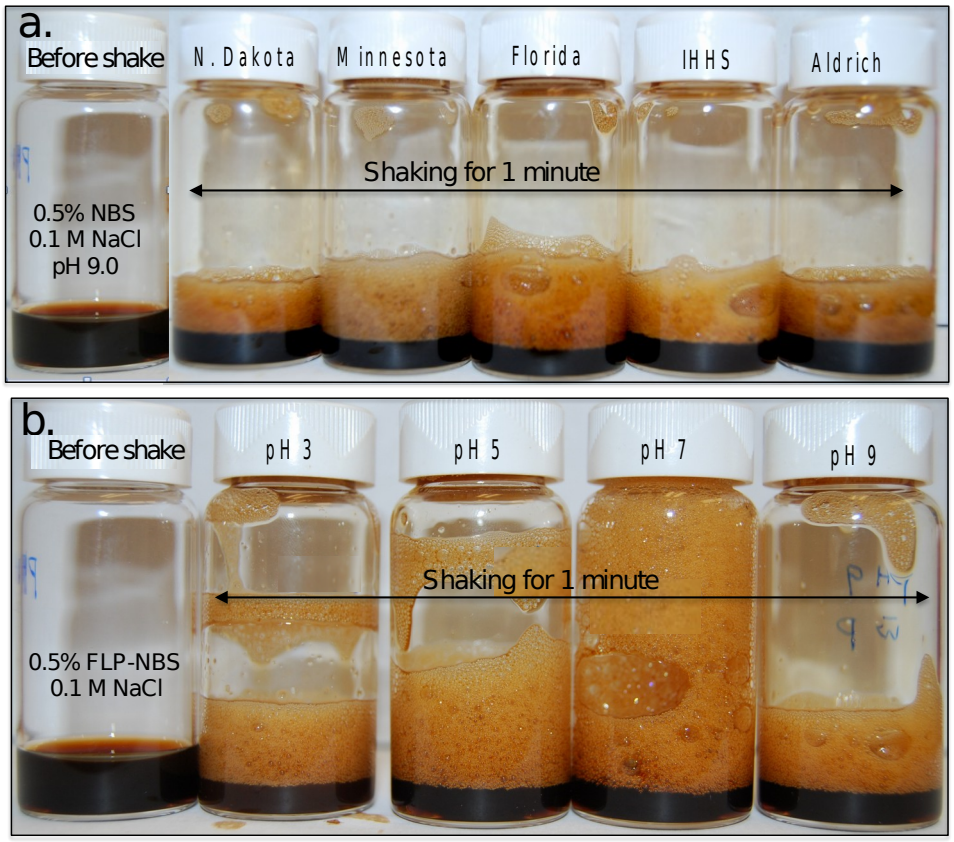

Figure 6. NBS air-in-water foams generated by shaking sealed 20 mL vials containing 2 ml NBS solution (remainder of the vial volume filled with air under atmospheric pressure. **(a)** Different NBS origins showed no significant differences in the resulting foam height. **(b)** The pH effect (using FLP-NBS), showing good pH tolerance. The left-most vial shows the NBS solution before shaking.

The FLP-NBS was used to generate $scCO_2$-in-water foams (although the air-in-water foam tests, Fig. 6a, suggested that the other NBS may behave similarly). From the generation of air-water foams, an NBS concentration of about 0.5% appeared optimal. Therefore, we selected three NBS concentrations to test: 0.1, 0.5, and 1.0% for the $scCO_2$-foam experiment. For foam quality, we targeted 80% to 83% CO_2, and found this range to be readily achievable. For generating and characterizing the $scCO_2$-water foams, the $scCO_2$ and NBS-solutions

were co-injected into the sand-packed column, after which the foam passed through the capillary tube viscometer (recording $\Delta P = P3 - P4$), and finally into the viewing chamber where the images of foam morphology were recorded (Figure 2). Apparent viscosities obtained with $scCO_2$ contents ranging from 80 to 83 % by volume, under different NBS concentrations in the aqueous phase, and a range of shear rates are shown in Figure 7. The co-injection rates ranged from 6 to 36 mL/min, with most rates ranging from 9 to 18 mL/min. The corresponding Darcy flow rates and residence times within the sandpack were 1.3×10^{-3} to 7.6×10^{-3} m/s, and 90 to 15 s, respectively. It should be noted that the associated shear rates in the capillary tube viscometer, ranging from 2,300 up to 13,900 s^{-1}, are very high. Given the typical shear-thinning behavior observed from these measurements (Figure 7), apparent viscosities under much lower shear rates of field injection processes are expected to be significantly higher than the value of 13 cP obtained at 2,300 s^{-1}. These tests collectively indicate that $scCO_2$-water foams are viable with 0.5 to 1.0 % NBS in the aqueous phase, and that the 0.1 % NBS concentration may be inadequate. More systematic experiments targeted to testing behavior at low shear rates are necessary to optimize the foam generation procedure and foam properties.

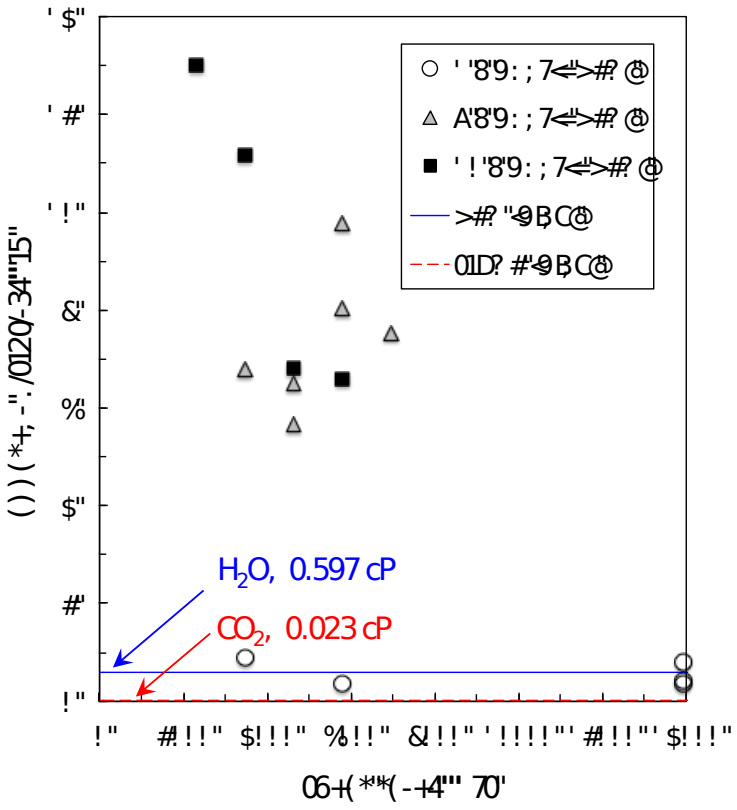

469

470**Figure 7.** Apparent viscosities of scCO$_2$-water foams (80 to 83 % CO$_2$
471by volume) at 8.5 to 9.0 MPa, for different concentrations of NBS in
472the aqueous phase. Viscosities of scCO$_2$ and H$_2$O are included for
473comparison.

474

475 Representative images of scCO$_2$-water foams using different
476NBS concentrations are presented in Figure 8. Although the NBS
477concentration of 0.1%, did not support high apparent viscosities
478under the tested very high shear rates, fairly consistent foams were
479generated, albeit with some mm-sized bubbles (Fig. 8a). The
480microscopic image of the 0.5% NBS case (inserted image in Fig. 8b)
481shows scCO$_2$ droplet sizes up to about 20 µm. When the NBS
482concentration was increased to 1.0% (Fig. 8c), the foam appeared
483mist-like. Example videos of foam flow through the viewing chamber
484are provided in the Supplemental Information.

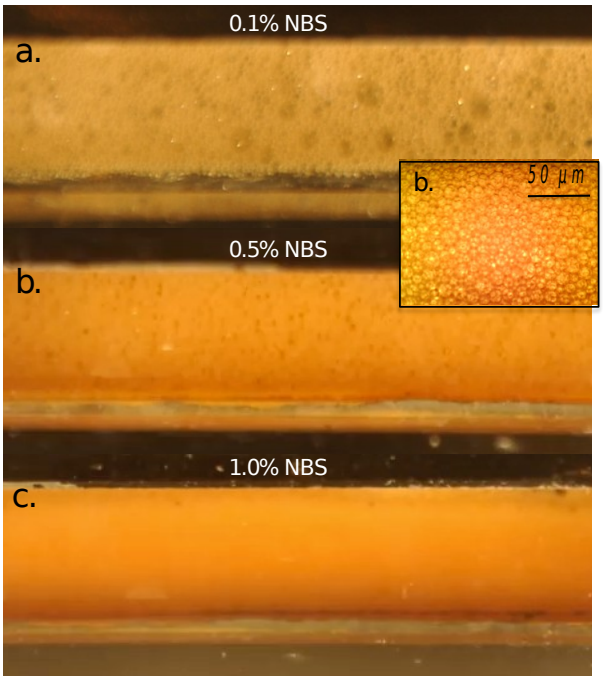

Figure 8. NBS generated $scCO_2$-in-water foams with 0.8 foam quality, and varied NBS concentrations (0.1, 0.5, and 1.0 %) and constant ionic strength 0.58% NaCl in the aqueous phase. No additional chemicals and additives were applied. The width of the viewing window is 15 mm.

SUMMARY

To evaluate the economic feasibility of NBS for industrial-scale subsurface engineering applications, the cost of NBS relative to synthetic surfactants currently used is a critical factor that needs further research. Although it is premature to make reliable production cost projections, the NBS are abundantly contained in humus deposits that are inexpensive and easily obtained. The cost of raw humus materials is only ~$25 per ton (not include the transportation). The laboratory bench scale extractions yielded an average ~17% NBS relative to the raw humus. The four common chemicals needed in

extraction include sodium hydroxide and hydrochloric acid (non-reusable), and benzene and methanol (recycled), and no costly synthesis and purification procedures are involved. Differences in origins of the humus appear to imparted no major differences in the chemical composition, structure, and function of the extracted NBS. Thus NBS appears to be potentially economically competitive. Our data show that NBS is effective for reducing interfacial tensions and for generating and stabilizing high quality air- and $scCO_2$-foams, indicating that it could be suitable for generating other types of foams and emulsions as well. Lastly, the benign nature of NBS will be an asset in reducing operational costs and environmental impacts.

ACKNOWLEDGEMENTS

This material is based upon work supported by (1) the Laboratory Directed Research and Development program (LDRD) of the Lawrence Berkeley National Laboratory (LBNL), and (2) the U.S. Department of Energy, Office of Fossil Energy, Office of Natural Gas and Petroleum Technology, through the National Energy Technology Laboratory (NETL), under Award Number DE-AC02-05CH11231 and FWP-ESD14085. Project management by Stephen Henry (NETL) is gratefully acknowledged. We thank the anonymous reviewers for their helpful comments.

References

1. (a) Gupta, D. V. S.; Bobier, D. M., The history and success of liquid CO2 and CO2/N2 frcturing system. In *SPE Gas Technology Symposium*, Society of Petroleum Engineers: Calgary, Alberta, Canada, 1998; p SPE 40016; (b) Wanniarachchi, W. A. M.; Ranjith, P. G.; Perera, M. S. A., Shale gas fracturing using foam-based fracturing fluid: a review. *Environ Earth Sci* **2017,** *76:91*; (c) Liu, H.; Wang, F.; Zhang, J.; Meng, S. W.; Duan, Y. W., Fracturing with carbon dioxide: Application status and development trend. *Petrol Explor Dev+* **2014,** *41* (4), 513-519.

5362. Enick, R. M.; Olsen, D. K. *Mobility and conformance control for* 537*carbon dioxide enhance oil recovery (CO_2-EOR) via thickeners, foams,* 538*and gels- A detailed literature review of 40 years of research*; National 539Energy Technology Laboratory: 2012; p 241.
5403. (a) Heller, J. P.; Dandge, D. K.; Card, R. J.; Donaruma, L. G. Direct 541Thickeners for Mobility Control of CO_2 Floods *SPE* [Online], 1985, p. 542679-686. https://www.onepetro.org/journal-paper/SPE-11789-PA; (b) 543Lee, J.; Dhuwe, A.; Cummings, S. D.; Beckman, E. J.; Enick, R. M.; 544Doherty, M.; O'Brien, M.; Perry, R.; Soong, Y.; Fazio, J.; McClendon, T. R. 545Polymeric and Small Molecule Thickeners for CO_2, Ethane, Propane, 546and Butane for Improved Mobility Control *SPE* [Online], 2016, p. 21. 547https://www.onepetro.org/conference-paper/SPE-179587-MS; (c) 548Trickett, K.; Xing, D. Z.; Enick, R.; Eastoe, J.; Hollamby, M. J.; Mutch, K. 549J.; Rogers, S. E.; Heenan, R. K.; Steytler, D. C., Rod-like micelles thicken 550CO_2. *Langmuir* **2010,** *26* (1), 83-88.
5514. (a) Nguyen, Q. P.; Alexandrov, A. V.; Zitha, P. L.; Currie, P. K., 552Experimental and modeling studies on foam in porous media: A review. 553*SPE* **2000,** (SPE 58799); (b) Heller, J. P., CO_2 foams in enhanced oil 554recovery. In *Foam: Fundamentals and Applications in the Petroleum* 555*Industry*, Schramm, L., Ed. American Chemical Society: Washington, 556DC, 1994; pp 201-234; (c) Johnston, K. P.; da Rocha, S. R. P., Colloids in 557supercritical fluids over the last 20 years and future directions. *Journal* 558*of Supercritical Fluids* **2009,** *47* (3), 523-530; (d) Hirasaki, G. J.; 559Lawson, J. B., Mechanisms of foam flow in porous media: Apparent 560viscosity in smooth capillaries. *SPE Journnal* **1985,** *April 1985*, 176-561190; (e) Falls, A. H.; Musters, J. J.; Ratulowski, J., The apparent viscosity 562of foams in homogeneous bead packs. *SPE Reservoir Engineering* 563**1989,** *May 1989*, 155-164; (f) Kovscek, A. R.; Tang, G. Q.; Radke, C. J., 564Verification of Roof snap off as a foam-generation mechanism in 565porous media at steady state. *Colloids and Surfaces A:* 566*Physicochemical Engineering Aspects* **2007,** *302*, 251-260; (g) Chen, 567M.; Yortsos, Y. C.; Rossen, W. R., Pore-network study of the 568mechanisms of foam generation in porous media. *Physical Review E* 569**2006,** *73* (036304), 1-20.
5705. (a) Adkins, S. S.; Chen, X.; Nguyen, Q. P.; Sanders, A. W.; 571Johnston, K. P., Effect of branching on the interfacial properties of 572nonionic hydrocarbon surfactants at the air-water and carbon dioxide-573water interfaces. *Journal of Colloid and Interface Science* **2010,** *346*, 574455-463; (b) Adkins, S. S.; Chen, X.; Chan, I.; Torino, E.; Nguyen, Q. P.; 575Sanders, A. W.; Johnston, K. P., Morphology and stability of CO_2-in-576water foams with nonionic hydrocarbon surfactants. *Langmuir* **2010,** 577*26* (8), 5335-5348; (c) Da, C.; Xue, Z.; Worthen, A. J.; Qajar, A.; Huh, C.; 578Prodanovic, M.; Johnston, K. P., Viscosity and stability of dry CO_2 foams 579for improved oil recovery. In *SPE Improved Oil Recovery Conference*, 580Society of Petroleum Engineers: Tulsa, OK, 2016; Vol. SPE-179690-MS; 581(d) Johnston, K. P.; Alzobaidi, S.; Da, S.; Tran, V., High temperature

582ultradry carbon dioxide-in-water foam stabilized with viscoelastic
583surfactants. In *AIChE Annual Meeting*, AIChE: San Francisco, CA, 2016;
584(e) Xue, Z.; Worthen, A. J.; Da, C.; Qajar, A.; Ketchum, I. R.; Alzobaidi,
585S.; Huh, C.; Prodanovic, M.; Johnston, K. P., Ultradry carbon dioxide-in-
586water foams with viscoelastic aqueous phases. *Langmuir* **2016,** *32* (1),
58728-37.
5886. Kosaric, N.; Vardar-Sukan, F., *Biosurfactants : production and*
589*utilization--processes, technologies, and economics*. CRC Press: Boca
590Raton, 2015.
5917. Stevenson, F. J., *Humus chemistry : genesis, composition,*
592*reactions*. 2nd ed.; Wiley: New York, 1994; p xiii, 496 p.
5938. Sutton, R.; Sposito, G., Molecular structure in soil humic
594substances: The new view. *Environ. Sci. Technol.* **2005,** *in press*.
5959. (a) Hayase, K.; Tsubota, H., Sedimentary humic and fulvic acid as
596surface active substances. *Geochimica et Cosmochimica Acta* **1983,**
597*47*, 947-952; (b) Chilom, G.; Bruns, A. S.; Rice, J. A., Aggregation of
598humic acid in solution: Contributions of different fractions. *Organic
599Geochemistry* **2009,** *40*, 455-460; (c) Aiken, G. R.; Mcknight, D. M.;
600Thorn, K. A.; Thurman, E. M., Isolation of Hydrophilic Organic-Acids
601from Water Using Nonionic Macroporous Resins. *Organic Geochemistry*
602**1992,** *18* (4), 567-573.
60310. (a) Tschapek, M.; Wasowski, C., The surface activity of humic
604acid. *Geochimica et Cosmochimica Acta* **1976,** *40*, 1343–1345; (b) Von
605Wandruszka, R., The micellar model of humic acid: evidence from
606pyrene fluorescence measurements. *Soil Science* **1998,** *163*, 921-930;
607(c) Tombácz, E., Colloidal properties of humic acids and spontaneous
608changes of their colloidal state under variable solution conditions. *Soil
609Science* **1999,** *164*, 814-824; (d) Guetzloff, T. F.; Rice, J. A., Does humic
610acid form a micelle? *The Science of the Total Environment* **1994,** *152*
611(31-35).
61211. Harwood, L. M.; Moody, C. J., *Experimental organic chemistry:*
613*Principles and Practice* Wiley-Blackwell: 1989.
61412. Jung, J. W.; Wan, J., Supercritical CO_2 and ionic strength effects on
615wettability of silica surfaces: Equilibrium contact angle measurements.
616*Energy and Fuels* **2012,** *26* (9), 6053−6059.
61713. Hart, J.; Ellenberger, J.; Hamersma, P. J., Single- and two-phase
618flow through helical coiled tubes. *Chem. Eng. Sci.* **1988,** *43* (4), 775-
619783.
62014. (a) Wu, Q.; Schleuss, U.; Blume, H. P., Investigation on Soil Lipid
621Extraction with Different Organic Solvents. *Angenommen* **1995,** *4*
622(Januar), 347-350; (b) Jeannotte, R.; Hamel, C.; Jabaji, S.; Whalen, J. K.,
623Comparison of solvent mixtures for pressurized solvent extraction of
624soil fatty acid biomarkers. *Talanta* **2008,** *77* (1), 195-199.
62515. (a) Jansen, B.; Nierop, K. G. J.; Kotte, M. C.; de Voogt, P.;
626Verstraten, J. M., The applicability of accelerated solvent extraction
627(ASE) to extract lipid biomarkers from soils. *Applied Geochemistry*

628**2006,** *21* (6), 1006-1015; (b) Quenea, K.; Mathieu, J.; Derenne, S., Soil
629lipids from accelerated solvent extraction: Influence of temperature
630and solvent on extract composition. *Org Geochem* **2012,** *44*, 45-52.
63116. (a) Wang, L. J.; Weller, C. L., Recent advances in extraction of
632nutraceuticals from plants. *Trends Food Sci Tech* **2006,** *17* (6), 300-
633312; (b) Marr, R.; Gamse, T., Use of supercritical fluids for different
634processes including new developments - a review. *Chem Eng Process*
635**2000,** *39* (1), 19-28; (c) Kaufmann, B.; Christen, P., Recent extraction
636techniques for natural products: Microwave-assisted extraction and
637pressurised solvent extraction. *Phytochem Analysis* **2002,** *13* (2), 105-
638113; (d) Luque-Garcia, J. L.; de Castro, L., Ultrasound: a powerful tool
639for leaching. *Trac-Trend Anal Chem* **2003,** *22* (1), 41-47.
64017. (a) Gostishcheva, M. V.; Belousov, M. V.; Yusubov, M. S.;
641Ismatova, R. R.; Dmitruk, S. E., Comparative IR spectral characteristics
642of humic acids from peats of different origin in the Tomsk area. *Pharm*
643*Chem J* **2009,** *43* (7), 418-421; (b) Senesi, N.; D'Orazio, V.; Ricca, G.,
644Humic acids in the first generation of EUROSOILS. *Geoderma* **2003,**
645*116* (3-4), 325-344; (c) Tatzber, M.; Stemmer, M.; Splegel, H.;
646Katziberger, C.; Haberhauer, G.; Mentler, A.; Gerzabek, M. H., FTIR-
647spectroscopic characterization of humic acids and humin fractions
648obtained by advanced NaOH, Na4P2O7, and Na2CO3 extraction
649procedures. *J Plant Nutr Soil Sc* **2007,** *170* (4), 522-529.
65018. Noll, L. A. *Ambient and high-temperature calorimetry of*
651*commercial surfactants*; National Institute for Petroleum and Energy
652Research: Bartlesville, OK, 1989; p 58.
65319. Vargaftik, N. B.; Volkov, B. N.; Voljak, L. D., International tables of
654the surface tension of water. *Journal of Physical and Chemical*
655*Reference Data* **1983,** *12* (3), 817-820.
65620. Bachu, S.; Bennion, D. B., Dependence of CO_2-brine interfacial
657tension on aquifer pressure, temperature and water salinity. *Energy*
658*Procedia* **2009,** *1*, 3157-3164.
65921. (a) Kim, Y.; Wan, J.; Kneafsey, T. J.; Tokunaga, T. K., Dewetting of
660silica surfaces upon reactions with supercritical CO_2 and brine: Pore-
661scale studies in micromodels. *Environmental Science & Technology*
662**2012,** *46*, 4228-4235; (b) Hu, R.; Wan, J. M.; Kim, Y.; Tokunaga, T. K.,
663Wettability effects on supercritical CO2-brine immiscible displacement
664during drainage: Pore-scale observation and 3D simulation.
665*International Journal of Greenhouse Gas Control* **2017,** *60*, 129-139.
666